Numerical investigation of the cavitational behaviour into a storage pump at off design operating points

2010 IOP Conf. Ser.: Earth Environ. Sci. 12 012068

(http://iopscience.iop.org/1755-1315/12/1/012068)

IOP Conf. Series: Earth and Environmental Science **12** (2010) 012068 doi:10.1088/1755-1315/12/1/012068

Numerical investigation of the cavitational behaviour into a storage pump at off design operating points

A Stuparu[1], R Susan-Resiga[1], L E Anton[1] and S Muntean[2]

[1]Department of Hydraulic Machinery, Politehnica University of Timisoara, Bd. Mihai Viteazu 1, Timisoara, 300222, Romania
[2]Centre of Advanced Research in Engineering Science, Romanian Academy-Timisoara Branch, Bd. Mihai Viteazu 24, Timisoara, 300223, Romania

E-mail: astuparu@mh.mec.upt.ro

Abstract. The paper presents a new method for the analysis of the cavitational behaviour of hydraulic turbomachines. This new method allows determining the coefficient of the cavitation inception and the cavitation sensitivity of the turbomachines. We apply this method to study the cavitational behaviour of a large storage pump. By plotting in semi-logarithmic coordinates the vapour volume versus the cavitation coefficient, we show that all numerical data collapse in an exponential manner. This storage pump is located in a power plant and operating without the presence of the developed cavitation is vital. We investigate the behaviour of the pump from the cavitational point of view while the pump is operating for variable discharge. A distribution of the vapour volume upon the blade of the impeller is presented for all the four operating points. It can be seen how the volume of vapour evolves from one operating point to another. In order to study the influence of the cavitation phenomena upon the pump, the evolution of the pumping head against the cavitation coefficient is presented. That will show how the pumping head drops while the cavitation coefficient decreases. From analysing the data obtained from the numerical simulation it results that the cavitation phenomena is present for all the investigated operating points. By analysis of the slope of the curve describing the evolution of the vapour volume against the cavitation coefficient we determine the cavitation sensitivity of the pump for each operating point. It is showed that the cavitation sensitivity of the investigated storage pump increases while the flow rate decreases.

1. Introduction

In many engineering applications, cavitation has been the subject of extensive theoretical and experimental research since it has predominantly been perceived as an undesirable phenomenon. This is mainly due to the detrimental effects of cavitation such as erosion, noise and vibrations, caused by the growth and collapse of vapour bubbles. The ability to model cavitating flows has drawn strong interest in CFD community. It covers a wide range of applications, such as pumps, hydraulic turbines, inducers and fuel cavitation in orifices as commonly encountered in fuel injection systems. Fluid machinery is a common application where low pressures are routinely generated by the machine action, e.g. on blade surfaces, with a consequent possibility of cavitation. Existence of cavitation is often undesired, because it can degrade the device performance, produce undesirable noise, lead to physical damage to the device and affect the structural integrity. Details of the existence, extent and effects of cavitation can be of significant help during the design stages of fluid machinery, in order to minimize cavitation or to account for its effects and optimize the design.

Past several decades have seen considerable research on cavitation and extensive reviews are available in the literature [1], [3]. Different aspects of this complex phenomenon have been explored, including, e.g., cavitation bubble collapse and erosion damage, cavitation acoustics, cloud cavitation and rotating cavitation.

Viscous flow models, which regard the cavitating flow as the bubbly flow containing spherical bubbles, were introduced to provide highly accurate calculations. In the viscous flow models, the Navier-Stokes equation including cavitation bubble is solved in conjunction with Rayleigh's equation governing the change in the bubble radius. To account for the cavitation dynamics in a more flexible manner a transport equation model has been

developed. In this approach volume or mass fraction of liquid (and vapour) phase is convective. Singhal et al. [5] have employed similar models based on this concept with differences in the source terms.

Hirschi et al. [8] proposed a method, which allows the performance drop prediction, consisting of assuming the cavity interface as a free surface boundary of the computation domain and that leads to compute only a single phase flow. The unknown shape of the interface is determined using an iterative procedure matching the cavity surface to a constant pressure boundary. The numerical results were in good agreement with the measurements. The originality of the method was that the adaptation process is done apart from the flow calculation, allowing the use of any numerical simulation software. Ait-Bouziad [11] used the mixture model for the case study of an industrial inducer and found that this model provides satisfactory results for the prediction of the cavitation flow behaviour and performance drop estimation. Pouffary et al. [9] investigate the cavitating flow in turbomachinery with the help of numerical simulation using a barotropic state law to model cavitation phenomenon. From the comparison of the numerical results with experiment a good agreement results regarding the head drop of the investigated turbomachines. Flores et al. [10] used a numerical model based on homogeneous approach of the multiphase flow coupled with a barotropic state law for the cool water vapour-liquid mixture. The numerical results showed a good prediction of the head drop and were compared with experimental results leading to a good overlapping.

This paper presents the computational analysis of the cavitational behaviour of a storage pump for off design operating points by using the new method for determining the cavitation inception coefficient and the curves describing the cavitation sensitivity. Two-phase cavitating flow models based on homogeneous mixture approach, with a transport equation for the vapour volume fraction have been included in expert commercial codes such as FLUENT [6] that we use. We conclude that, for steady cavitating flow, the model presented in this paper, captures correctly the vapour phase distribution on the blade of the pump impeller. The current effort is based on the application of the full cavitation model that utilizes the modified Rayleigh-Plesset equations for bubble dynamics and includes the effects of turbulent pressure fluctuations and non-condensable gases (ventilated cavitation) to rotating cavitation in different types of fluid turbomachines.

2. Numerical method of modelling cavitating flow

The FLUENT code employs a generally applicable predictive procedure for turbulent two-phase cavitating flows developed by Cokljat et al. [3]. This model enables formation of vapour from liquid when the pressure drops below the vaporization pressure. If α_V is the vapour volume fraction, then the continuity equation for the vapour phase is,

$$\frac{\partial}{\partial t}\left(\alpha_V \rho_V\right) + \nabla \cdot \left(\alpha_V \rho_V \vec{u}_V\right) = \dot{m}_V \tag{1}$$

where $\vec{u}_V$ is the velocity of the vapour phase, ρ_V is the vapour density, and $\dot{m}_V$ is the rate of liquid-vapour mass transfer. Obviously, the liquid volume fraction is

$$\alpha_l = 1 - \alpha_V \tag{2}$$

and mixture density and viscosity are defined below:

$$\rho_m = \left(1 - \alpha_V\right)\rho_l + \alpha_V \rho_V \tag{3}$$

$$\mu_m = \left(1 - \alpha_V\right)\mu_l + \alpha_V \mu_V . \tag{4}$$

The continuity equation for the liquid phase is:

$$\frac{\partial}{\partial t}\left(\alpha_l \rho_l\right) + \nabla \cdot \left(\alpha_l \rho_l \vec{u}_l\right) = -\dot{m}_V \tag{5}$$

Adding eq. (5) to eq. (1) the mixture continuity equation is obtained:

$$\frac{\partial \rho_m}{\partial t} + \nabla \cdot \left(\rho_m \vec{u}_m\right) = 0 \tag{6}$$

where the mixture velocity is defined by:

$$\rho_m \vec{u}_m = \left(1 - \alpha_V\right)\rho_l \vec{u}_l + \alpha_V \rho_V \vec{u}_V \tag{7}$$

Assuming homogeneous multiphase flow, with no slip between the phases, the same velocity field is shared

among the phases:

$$\vec{u}_m = \vec{u}_V = \vec{u}_l \tag{8}$$

This assumption is motivated in the cavitation model because no interface between the liquid and vapour phases is assumed, thus allowing the fluids to be interpenetrating. The conservation equation for momentum (with negligible body forces) is:

$$\frac{\partial}{\partial t}\left(\rho_m \vec{u}_m\right) + \nabla \cdot \left(\rho_m \vec{u}_m \vec{u}_m\right) = -\nabla p_m + \nabla \cdot \mu_m \left[\nabla \vec{u}_m + \left(\nabla \vec{u}_m\right)^T\right] \tag{9}$$

Since the cavitation bubble grows is a liquid at low temperature the latent heat of evaporation can be neglected and the system can be considered isothermal. Under these conditions the pressure inside the bubble remains practically constant and the growth of the bubble radius, R, can be approximated by the simplified Rayleigh equation:

$$\frac{dR}{dt} = \sqrt{\frac{2\left(p_{vap} - p\right)}{3\rho_l}} \tag{10}$$

where p_{vap} is the pressure of vaporization and ρ_l is the liquid density. The total mass of vapour per mixture volume unit can be written as:

$$m_V = \rho_V \frac{4}{3}\pi R^3 n_b \tag{11}$$

with n_b is the bubble number density. It results,

$$\dot{m}_V = \frac{dm_V}{dt} = \frac{3\rho_V \alpha_V}{R}\frac{dR}{dt} = \frac{3\rho_V \alpha_V}{R}\sqrt{\frac{2\left(p_{vap} - p\right)}{3\rho_l}} \tag{12}$$

with bubble radius given by:

$$R = \left(\frac{\alpha_V}{\frac{4}{3}\pi n_b}\right)^{1/3} \tag{13}$$

Bernad et al. [2] suggest a minimum of 10^4 and maximum of 10^6 values for the bubble density number n_b. However, in [2] it shows that the bubble initial radius has an insignificant influence on the final radius, as well as on the time for bubble growing up along streamlined bodies. As a result, when a steady cavitating flow configuration is computed, the bubble density number should have little influence on the final result.

The FLUENT code requires the following methodology for computing cavitating flows. First, a steady solution is obtained for a single phase (liquid) flow, solving eq. (6) and eq. (9). Second, the cavitation model is turned on and the steady equations are solved, with the vapour volume fraction, and therefore the liquid-vapour mixture density, as an additional unknown.

Physically, the cavitation process is governed by thermodynamics and kinetics of the phase change process. The liquid-vapour conversion associated with the cavitation process is modelled through two terms, which represents, respectively, condensation and evaporation.

3. Numerical approach, computational domain and boundary conditions

To simulate the cavitating flow the numerical code FLUENT [6] was used. The code uses a control volume-based technique to convert the governing equations in algebraic equations that can be solved numerically. This control volume technique consists of integrating the governing equations at each control volume, yielding discrete equations that conserve each quantity on a control-volume basis. The governing integral equations for the conservation of mass and momentum, and (when appropriate) other scalars, such as turbulence, are solved sequentially. Being the governing equations non-linear (and coupled), several iterations of the solution loop must be performed before a converged solution is obtained. The flow solution procedure is the SIMPLE routine [6]. This solution method is designed for incompressible flows, thus being semi-implicit. The full Navier-Stokes equations are solved. The flow was assumed to be steady, and isothermal. In these calculations turbulence effects were considered using turbulence models, as the k-ε RNG models, with the modification of the turbulent

viscosity for multiphase flow. To model the flow close to the wall, enhanced wall functions approach has been used to model the near-wall region (i.e., laminar sub layer, buffer region, and fully-turbulent outer region). For this model, the used numerical scheme of the flow equations was the segregated implicit solver. The SIMPLE scheme was employed for pressure-velocity coupling, first-order up-wind for the momentum equations and for other transport equations (e.g. vapour transport and turbulence modelling equations). Computational domain is meshed using the GAMBIT pre-processor [6].

The computational domain includes the impeller of the storage pump. For the numerical investigation only one inter-blade channel is used because of the symmetry of the geometry, Fig. 1a.

a) b)

Fig. 1 a)Impeller of the storage pump with highlighted inter blade channel
b) Mesh generated on the 3D computational domain of the inter-blade channel

The inter-blade channel domain is meshed with 322726 cells using a structured mesh, see Fig. 1b. On the inl et surface of the impeller, for the liquid phase, a constant velocity field was imposed normal on the surface. The velocity magnitude is computed using the flow rate of the operating point:

$$v_{l\_IN} = \frac{Q}{S_{IN}} \tag{14}$$

On the outlet surface a constant value of the pressure is imposed. Then, the pressure is lowered slowly down to the value corresponding to the desired cavitation number σ defined as:

$$\sigma = \frac{p_{m\_IN} - p_{vap}}{\rho_m g H} \tag{15}$$

Vapour appears during the pressure decrease. After obtaining a steady single phase (liquid) flow solution, FLUENT 6.3 code allows turning on the cavitation model. As a consequence, vapour formation is enabled where the absolute pressure is smaller than the vaporization pressure, p_{vap}. In order to obtain correct results the operating pressure, p_{op}, must be set to zero (by default is equal with the atmospheric pressure), therefore the gauge pressure, p_{gauge}, will be equal with the absolute pressure, p_{abs}:

$$p_{abs} = p_{op} + p_{gauge} \tag{16}$$

This setting is important for obtaining only positive absolute pressure values.

On the periodic surfaces of the impeller the periodicity of the velocity, pressure and turbulence parameters were imposed:

$$p(r,\theta,z) = p\left(r,\theta+\frac{2\pi}{n_p},z\right) \tag{17}$$

$$\vec{v}(r,\theta,z) = \vec{v}\left(r,\theta+\frac{2\pi}{n_p},z\right) \tag{18}$$

$$k(r,\theta,z) = k\left(r,\theta+\frac{2\pi}{n_p},z\right) \tag{19}$$

$$\varepsilon(r,\theta,z)=\varepsilon\left(r,\theta+\frac{2\pi}{n_p},z\right) \tag{20}$$

The remaining boundary conditions for the impeller domain correspond to zero relative velocity on the blade, crown and hub. Figure 2 shows the 3D computational domain with boundary conditions corresponding to an inter-blade channel of the impeller. The computational domain is bounded upstream by an annular section (wrapped on the same annular surface as the suction outlet section, but different in angular extension) and extends downstream up to cylindrical patch, in order to impose the boundary conditions on the outlet section.

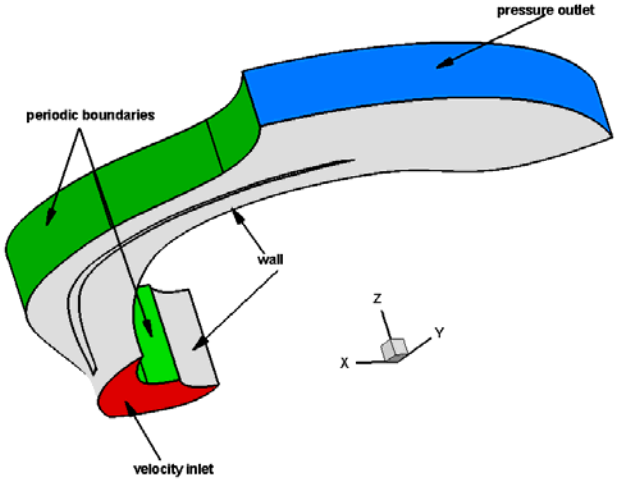

Fig. 2 Boundary conditions on the computational domain

We investigated the storage pump operating at 4 off design operating points with the characteristics given in the Tab.1:

Table 1 Values of the main characteristics for the operating points

Operating points	n [rot/min]	Q [m^3/s]	H [m]
OP1	1500	0.8	350
OP2		0.9	337
OP3		1.1	300
OP4		1.2	265

4. Numerical results

In order to compute the pumping head the following equation is used:

$$H=\frac{p_{m\_OUT}-p_{m\_IN}}{\rho_m g}+\frac{v^2_{m\_OUT}-v^2_{m\_IN}}{2g}+z_{OUT}-z_{IN} \tag{21}$$

If the total pressure is given by:

$$p_{m\_tot}=p_m+\frac{\rho_m v_m^2}{2} \tag{22}$$

and the difference between the inlet and outlet position is negligible then the pumping head has the following expression:

$$H=\frac{p_{m\_tot\_OUT}-p_{m\_tot\_IN}}{\rho_m g}=\frac{\Delta p_{m\_tot}}{\rho_m g} \tag{23}$$

The suction head is determined with the equation:

$$H_s = \frac{p_{atm} - p_{tot\_IN}}{\rho_m g} \tag{24}$$

The cavitation number of the installation is calculated using the equation:

$$\sigma_{inst} = \frac{\frac{p_{atm}}{\rho g} - \frac{p_V}{\rho g} - H_s}{H} \tag{25}$$

And the volume of vapour is given by

$$V_V = \int V_V dV = \sum_{i=1}^{n} V_{Vi} |V_i| \tag{26}$$

Figure 3 underlines the pumping head drop due to the decreasing of the cavitation number of the installation for the numerically investigated operating points. It can be observed that when a critical value of the σ_{inst} is reached, an abrupt drop of the pumping head occurs for all four regimes.

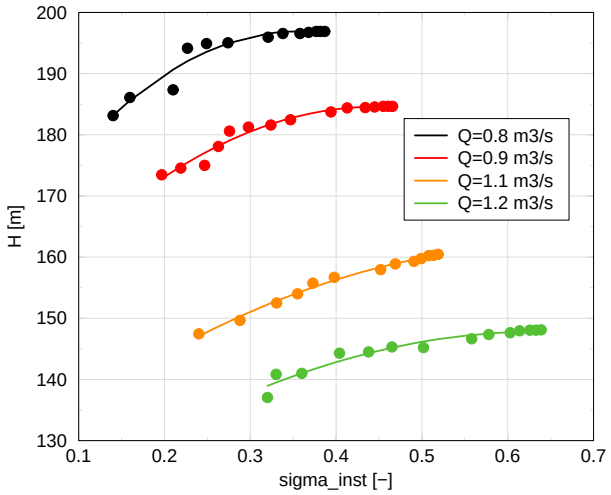

Fig. 3 Pumping head drop due to cavitation phenomena

Because the connection between the volume of vapour and the flow rate is given by the following equation:

$$V_V = A\,exp(B\sigma_{inst}) \tag{27}$$

where A, B are two coefficients specific for every operating point, the interdependency of the volume of vapour and the flow rate was represented using a semi-logarithmic plot, applying the next equation:

$$lg\,V_V = lg\,A + B\sigma_{inst} \tag{28}$$

From the numerical simulation of the multiphase flow for the 4 operating points of the storage pump we obtained the following results describing the variation of the vapour volume as a function of the cavitation number of the installation, Fig. 4a-d:

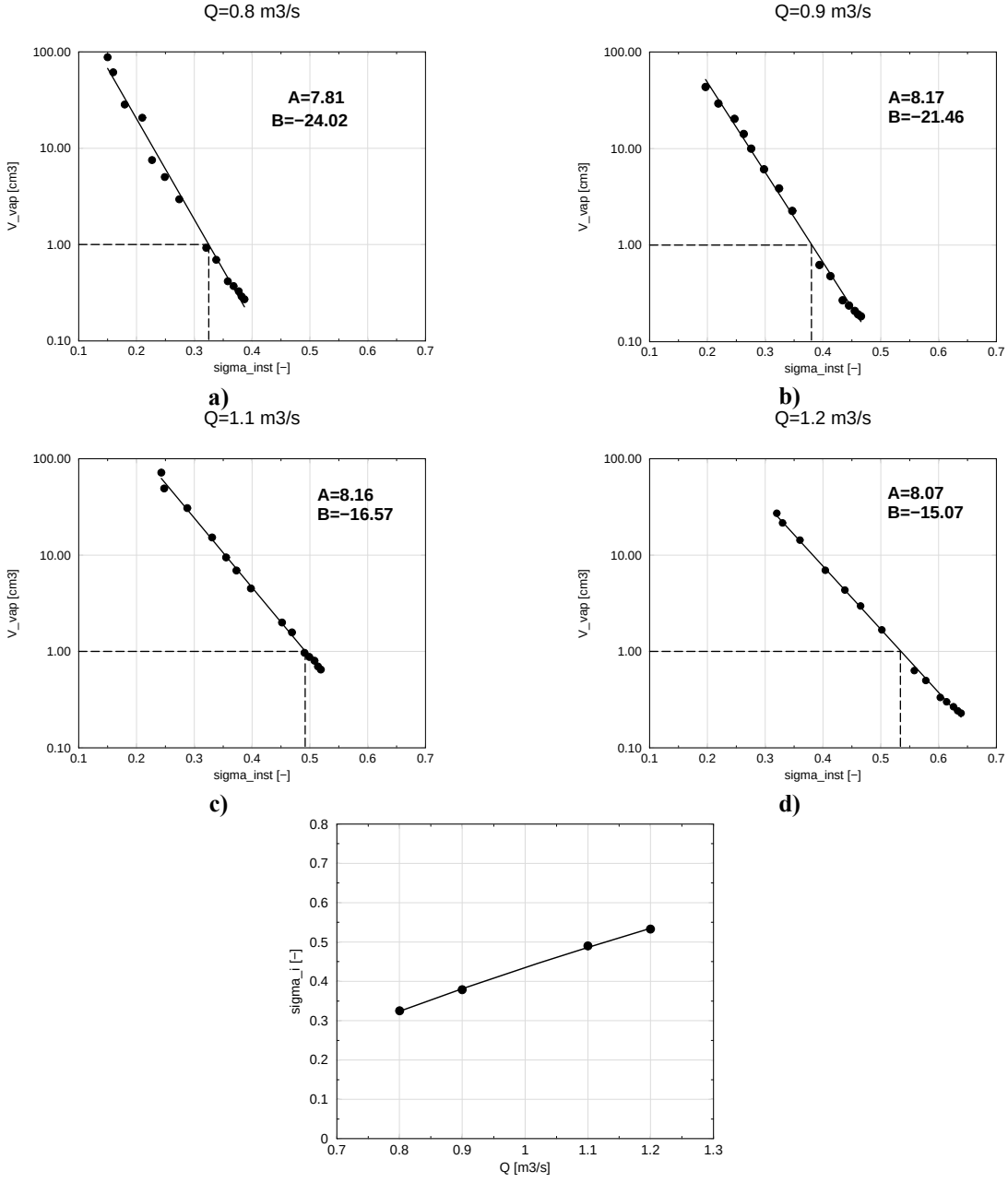

Fig. 4 a)-d)Variation of the volume of vapour against the cavitation number for the investigated operating points e) Evolution of the incipience cavitation number as a function of flow rate

In order to determine the cavitation incipience coefficient, it was considered, according to our new theory that the volume of vapour of 1 cm^3 corresponds to the volume of the first bubble, so the cavitation coefficient corresponding to this value of the volume of vapour represents the cavitation incipience coefficient. From Fig. 4a-d it results that for the operating point OP1 the cavitation incipience coefficient is equal with σ_i=0.32, for operating point OP2, σ_i=0.38, for operating point OP3, σ_i=0.49 and for operating point OP4, σ_i=0.53. This new theory allows us also to compare the cavitational behavior of the same pump operating at variable discharge or of different pumps operating at the same discharge by comparing the slope of the curves represented in Fig. 4. A higher value of the slope of the curve represents a higher cavitation sensitivity of the pump impeller, while a smaller value of the slope of the curve predicts lower cavitation sensitivity. So, if one has obtained the curves describing the cavitational behavior of a hydraulic turbomachines, not just a pump, it can easily determine, by

comparison of these curves, which turbomachines has a better cavitational behavior. For the centrifugal pump investigated it results from Fig. 4a-d that the slope of the curve increases with the decrease of the flow rate. That shows that the cavitational behavior of the investigated pump is getting worse while the flow rate decreases.

From Fig. 4e it results that the value of the cavitation inception coefficient increases with the value of the flow rate.

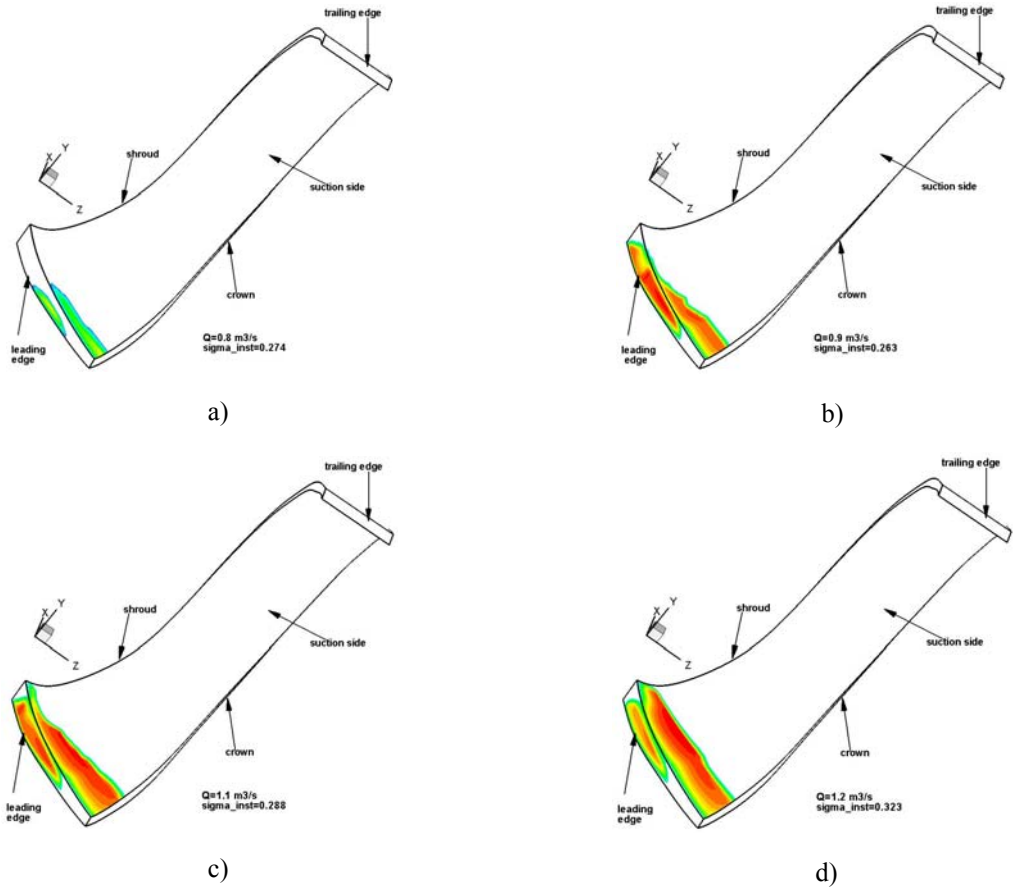

Fig. 5 Distribution of the volume of vapour on the suction side of the blade for different operating points

Analysing Fig. 5 and Fig. 4 it results that for all investigated operating points the developed cavitation is pres ent on the suction side of the impeller blade. From Fig. 5 it can be observed that while the flow rate is increasing, so that the contra pressure on the inlet of the pump will be smaller, the cavitation phenomena it develops mor e and more. Initially, the volume of vapour is present only on a small part of the leading edge and in its vicinity o n the suction side, but its size grows while the flow rate rises and in the end is present on almost 2/3 of the leadin g edge and on a great part of the suction side of the blade.

5. Conclusions

In this paper we use standard software with an implemented cavitation model, in order to obtain the necessary data for the construction of the cavitation curves witch allows use to determine the cavitational behaviour of a centrifugal storage pump. A new and robust method for the determination for the cavitation inception coefficient and cavitational behaviour of a centrifugal pump is presented. By using this method one can determine with good precision the value of the cavitation inception coefficient and the cavitational characteristic for hydraulic turbomachines. We apply this new method for analysing the cavitational behaviour of a large centrifugal storage pump. It results that the value of the cavitation inception coefficient increases while the flow rate increases, while the cavitation sensitivity of the centrifugal pump is getting higher with the decreasing of the flow rate.

The analyse of the results of the numerical investigation of the multiphase flow inside the storage pump underlines the pumping head drop due to the development of cavitation phenomena, while the level of the water from the suction lake drops, for all four operating points. It is obviously that, while the cavern filled with vapour grows, the perturbation of the flow on the suction side of the blade is more accentuated, leading to the detachment of the flow from the blade, the decreasing of the deviation realised by the impeller blades, and consequently to the pumping head drop. On the other hand, the growth of the boundary layer on the suction side of the blade and the detachment of the flow leads to the increase of the hydraulic losses and the decrease of the hydraulic efficiency of the impeller. The cavitation phenomenon appears due to the unfavourable hydrodynamics generated by the geometric shape of the impeller blades, the leading edge of the blades being very sharp. In order to avoid the appearance of cavitation it is necessary to redesign the impeller with modern design methods and software.

Acknowledgements

Dr. Sebastian Muntean was supported by the Romanian Academy program “Hydrodynamics Optimization and Flow Control of the Hydraulic Turbomachinery in order to Improve the Energetic and Cavitational Performances”.

Nomenclature

g	gravitational acceleration [m/s^2]
H	pumping head [J/N]
H_s	suction head [J/N]
k	turbulent kinetic energy [m^2/s^2]
$\dot{m}_V$	rate of liquid-vapour mass transfer [kg/(s.m^{-3})]
m_V	total mass of vapour per viscosity liquid-vapour mixture [kg/(s.m^{-3})]
n	rotational speed [rot/min]
n_b	number of bubbles per volume fraction density unit volume of liquid [1/m^3]
n_p	number of blades [-]
p_m	liquid-vapour mixture pressure [Pa]
p_{m_tot}	liquid-vapour mixture total pressure [Pa]
p_{abs}	absolute pressure [Pa]
p_{atm}	atmospheric pressure [Pa]
p_{gauge}	gauge pressure [Pa]
p_{op}	operating pressure [Pa]
p_{m_IN}	inlet liquid-vapour mixture pressure [Pa]
p_{m_OUT}	outlet liquid-vapour mixture pressure [Pa]
$p_{m\_tot\_IN}$	inlet liquid-vapour mixture total pressure [Pa]
$p_{m\_tot\_OUT}$	outlet liquid-vapour mixture total pressure [Pa]
p_{vap}	vaporization pressure [Pa]
Q	flow rate [m^3/s]
r	radial coordinate [m]
R	bubble radius [m]
t	time [s]
$\vec{u}_m$	liquid-vapour mixture velocity [m/s]
v_{l_IN}	inlet liquid phase velocity [m/s]
v_{m_IN}	inlet liquid-vapour mixture velocity [m/s]
$\vec{u}_l$	liquid phase velocity [m/s]
$\vec{u}_V$	vapour phase velocity [m/s]
v_{m_OUT}	outlet liquid-vapour mixture velocity [m/s]
V_V	volume of vapour [cm^3]
z	axial coordinate [m]
z_{IN}	inlet position [m]
z_{OUT}	outlet position [m]
α_l	liquid volume fraction [-]
α_V	vapour volume fraction [-]
ε	dissipation rate [m^2/s^2]
μ_m	liquid-vapour mixture viscosity [kg/m.s]
μ_l	liquid volume fraction [kg/m.s]
μ_V	vapour volume fraction volume viscosity [kg/m.s]
ρ_m	liquid-vapour mixture density [kg/m^3]
ρ_l	liquid volume fraction density [kg/m^3]
ρ_V	vapour volume fraction density [kg/m^3]
σ	cavitation number [-]
σ_{inst}	cavitation number of the installation [-]
σ_i	inception cavitation number [-]
ϕ	angular coordinate [rad]

References

[1] Anton I 1985 *Cavitation* (Bucharest: Romanian Academy Publishing House) **2** (in Romanian)
[2] Bernad S, Resiga R, Muntean S and Anton I 2007 Cavitation Phenomena in Hydraulic Valves. Numerical Modelling *Proc. of the Roman. Acad.* A **8(2)**
[3] Cokljat D, Ivanov V A and Vasquez S A 1998 Two-Phase Model for Cavitating Flows *Proc. of the Third Int. Conf. on Multiphase Flow* (Lyon, France) p 224
[4] Li S C 2000 *Cavitation of Hydraulic Machinery* (Imperial College Press)
[5] Singhal A K, Vaidya N and Leonard A D 1997 Multi-Dimensional Simulation of Cavitating Flows Using a PDF Model for Phase Change *ASME FED Meeting* (Vancouver: Canada) p 3272
[6] *** 2002 *FLUENT 6.3 User's Guide Fluent Incorporated*
[7] Susan-Resiga R, Muntean S, Bernad S and Anton I 2003 Numerical investigation of 3D cavitating flow in Francis turbines *Proc. of the Int. Conf. on Modell. Fl. Flow (CMFF03)* (Budapest, Hungary) **2** pp 950-57
[8] Hirschi R, Dupont P H, Avellan F, Favre J N, Guelich J F and Parkinson E 1998 Centrifugal pump performance drop due to leading edge cavitation: numerical predictions compared with model tests *J. of Fluids Engin.* **120(6)** 705–11
[9] Pouffary B, Patella R F, Rebound J L and Lambert P A 2008 Numerical Simulation of 3D Cavitating Flows: Analysis of Cavitation Head Drop in Turbomachinery *J. of Fluids Engin.* **130** 061301-1 – 061301-10
[10] Gonzalo Flores N, Goncalves E, Fortes Patella R, Rolland J and Rebattet C 2008 Head Drop of a Spatial Turbopump Inducer *J. of Fluids Engin.* **130** p 111301
[11] Ait-Bouziad Y 2006 *Physical Modelling of Leading Edge Cavitation: Computational Methodologies and Application to Hydraulic Machinery* PhD Thesis (EPFL, Lausanne, Switzerland)